Rationalizing the Reactivity of Mixed Allyl Rare-Earth Borohydride Complexes with DFT Studies

Sami Fadlallah, Jashvini Jothieswaran, Iker Del rosal, Laurent Maron, Fanny Bonnet, Marc Visseaux

To cite this version:

Sami Fadlallah, Jashvini Jothieswaran, Iker Del rosal, Laurent Maron, Fanny Bonnet, et al.. Rationalizing the Reactivity of Mixed Allyl Rare-Earth Borohydride Complexes with DFT Studies. Catalysts, 2020, 10, pp.820. 10.3390/catal10080820 . hal-02926044

HAL Id: hal-02926044

https://hal.univ-lille.fr/hal-02926044v1

Submitted on 31 Aug 2020

catalysts

MDPI

Article

Rationalizing the Reactivity of Mixed Allyl Rare-Earth Borohydride Complexes with DFT Studies

Sami Fadlallah [1], Jashvini Jothieswaran [1], Iker Del Rosal [2], Laurent Maron [2,*], Fanny Bonnet [3,*] and Marc Visseaux [1,*]

[1] Univ. Lille, CNRS, Centrale Lille, Centrale Lille, Univ. Artois, UMR 8181—UCCS—Unité de Catalyse et Chimie du Solide, F-59000 Lille, France; sami.fadlallah@agroparistech.fr (S.F.); jashvinij@gmail.com (J.J.)
[2] Institut National des Sciences Appliquées, LPCNO (IRSAMC), Université de Toulouse, INSA, UPS, CNRS (UMR 5215), 135 Avenue de Rangueil, F-31077 Toulouse, France; idel_ros@insa-toulouse.fr
[3] Univ. Lille, CNRS, INRAE, Centrale Lille, UMR 8207—UMET—Unité Matériaux et Transformations, F-59000 Lille, France
* Correspondence: Laurent.maron@irsamc.ups-tlse.fr (L.M.); fanny.bonnet@univ-lille.fr (F.B.); marc.visseaux@univ-lille.fr (M.V.)

Received: 1 July 2020; Accepted: 19 July 2020; Published: 22 July 2020

Abstract: The reactivity of rare-earth complexes RE$(BH_4)_2(C_3H_5)(THF)_x$ (RE = La, Nd, Sm, Y, Sc) toward the Ring-Opening Polymerization (ROP) of ε-caprolactone (ε-CL) was rationalized by Density Functional Theory (DFT) calculations. Even if the polymerization reaction can be initiated by both RE-(BH_4) and RE-allyl bonds, experimental investigations have shown that the initiation via the borohydride ligand was favored, as no allyl group could be detected at the chain-end of the resulting polymers. DFT studies could confirm these observations, as it was highlighted that even if the activation barriers are both accessible, the allyl group is not active for the ROP of ε-CL due to the formation of a highly stable intermediate that disfavors the subsequent ring-opening.

Keywords: rare earth; allyl; borohydride; ring-opening polymerization; cyclic esters; DFT

1. Introduction

The Ring-Opening Polymerization (ROP) of cyclic esters was recently studied by means of RE$(BH_4)_2(C_3H_5)(THF)_x$ complexes (RE = La, Nd, Sm, Y, Sc) [1,2]. These complexes display two potentially active ligands toward nucleophilic reactivity, i.e., the borohydride and the allyl groups [3]. Borohydride complexes of the rare-earth elements are well known as efficient initiators for the ROP of ε-caprolactone (ε-CL) [4], as well as lactide [5–7] and other cyclic esters [8,9]. The resulting polyesters display a telechelic dihydroxy (lactone, lactide), aldehyde-hydroxy (lactide) or cyclic (lactone or lactide) molecular structure following polymerization mechanisms that are well established [10–15].

On the other hand, several studies have dealt with the ROP of cyclic esters initiated by rare-earth allyl complexes [16–19], where the polymer chain end-group is expected to be of the allyl type.

By using the mixed allyl–borohydride RE$(BH_4)_2(C_3H_5)(THF)_x$ complexes as initiators of lactone or lactide ROP, the polymerization may proceed either via allyl or borohydride initiation, as shown in Scheme 1.

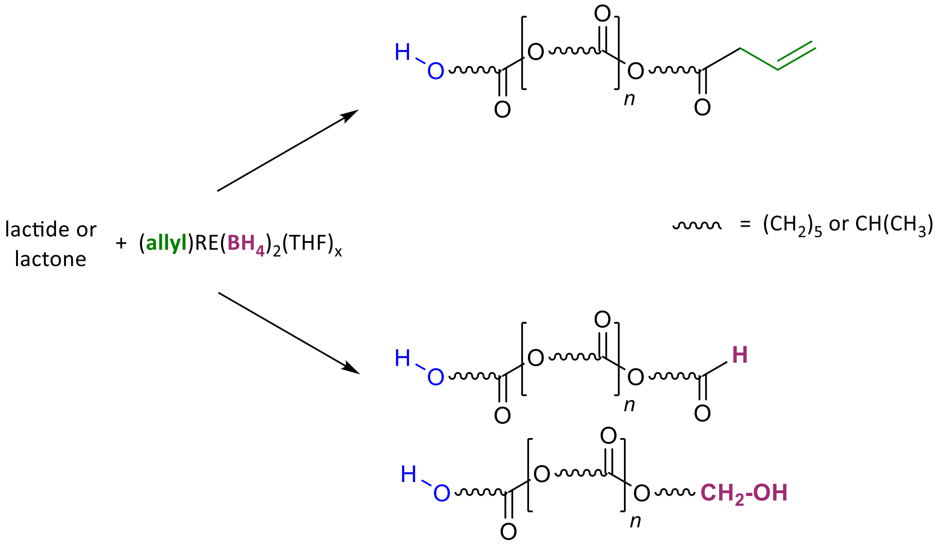

Scheme 1. The polymer end-groups expected from lactone/lactide Ring-Opening Polymerization (ROP) with mixed $RE(BH_4)_2(C_3H_5)(THF)_x$ complexes (ε-caprolactone taken here as an example).

Such a behavior of dual initiation ability is rather scarce in the literature. To our knowledge, one unique example to mention regarding the ROP of cyclic esters is the work of Okuda et al., who recently [20] showed that when the mixed alkyl–borohydride complex $[Y(Me)(BH_4)(thf)_5][BPh_4]$ (synthesized in [21]) is used as the initiator, the ROP of ε-CL can be promoted by either the borohydride or the methyl ligand, with comparable occurrences, based on DFT calculations. By replacing in silico the BH_4 by a dimethylamido ligand (thus considering the $[Y(Me)(NMe_2)(thf)_5]^+$ cation), the initiation is computed to take place preferentially through the methyl group and in a more facile way. This was attributed to a *trans* effect.

In our case, we could establish that the borohydride ligand initiates the polymerization at the expense of the allyl ligand, thanks to the ^{1}H NMR analysis of intentionally prepared low M_n polylactides that display signals relative to dihydroxytelechelic- or aldehyde-terminated macromolecules. Moreover, no allyl signals could be detected as the end-groups on these polymers, which excludes the occurrence of the initiation of the polymerization reaction via the Ln-allyl bond.

These results could be confirmed by Maldi-ToF analysis of low molecular weight polylactides, displaying a major population of aldehyde-terminated polylactide for the polymer synthesized with the neodymium complex and a major population of dihydroxytelechelic polylactide for the one synthesized with the yttrium analog, while no allyl-terminated polylactide could be observed in either case (see Figures S1 and S2). Another minor population of methoxy-terminated polylactide could be observed in both cases, which was attributed to the opening of cyclic polylactide by methanol when the reaction was quenched with the alcohol.

In order to tentatively rationalize this peculiar reactivity due to the presence of two possibly reactive groups on the same metal, we conducted a study in the form of a two-pronged approach. First, we explored the reactivity of such mixed allyl–borohydride complexes toward small molecules by ^{1}H NMR monitoring in order to observe, or not, a preference for the reactivity of one or the other ligand, and tentatively confirm, or not, the features observed in our experimental results of the ROP of cyclic esters. Second, a theoretical study was undertaken by means of Density Functional Theory (DFT) methods in order to weigh up each of the possibilities of reactivity and to deduce, or not, an understanding of the facts observed on an experimental scale.

2. Results and Discussion

2.1. ^{1}H NMR Monitoring Experiments

The reactions of the mixed allyl–borohydride complexes with benzophenone, tetramethyl- and tetramethylethylcyclopentadiene, dimethylanilinium tetraphenylborate and phenylsilane (Scheme 2) were monitored by ^{1}H NMR. The idea was to see which of the two reactivities, allyl or borohydride, if any, was taking place. To this end, we selected this set of small substrates for which the reactivity was already known for each of these functionalities.

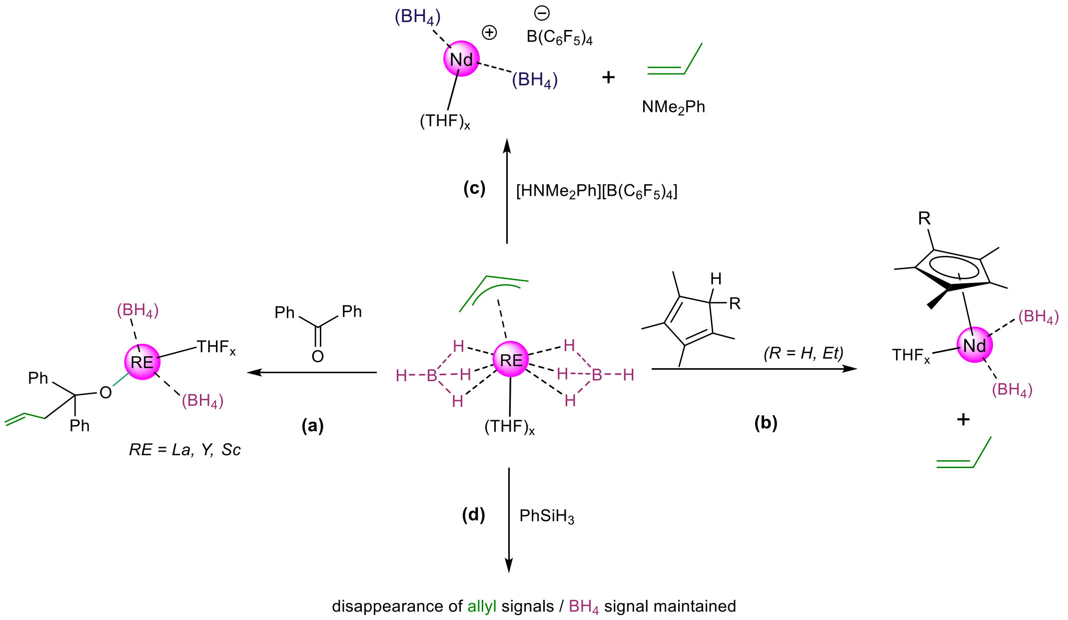

Scheme 2. Reactivity of RE(BH$_4$)$_2$(C$_3$H$_5$)(THF)$_x$ (RE = La, Y, Sc) complexes toward small molecules.

It is known that benzophenone can insert into an RE–allyl bond, as previously shown by Okuda et al. [22]. On the other hand, a ketone is also able to insert into an RE–borohydride bond to give the corresponding alkoxide [23]. By adding one equiv. of Ph$_2$CO to a THF-D$_8$ solution of RE(BH$_4$)$_2$(C$_3$H$_5$)(THF)$_x$ (RE = La, Y, Sc), we found by ^{1}H NMR that benzophenone reacts exclusively with the RE–(allyl) moiety, leading to the corresponding allyldiphenylalkoxide compound (Scheme 2, path a). Furthermore, the addition of one equivalent of substituted cyclopentadiene (C$_5$Me$_4$RH, R = H or Et) to Nd(BH$_4$)$_2$(C$_3$H$_5$)(THF)$_x$ afforded the immediate formation of the corresponding half-sandwich of the formula (C$_5$Me$_4$R)Nd(BH$_4$)$_2$ (Scheme 2, path b) [24], as unambiguously observed by ^{1}H NMR monitoring in C$_6$D$_6$. The reaction of Nd(BH$_4$)$_2$(C$_3$H$_5$)(THF)$_x$ with one equiv. of [HNMe$_2$Ph][B(C$_6$F$_5$)$_4$] in THF-D$_8$ gave the already reported [Nd(BH$_4$)$_2$][B(C$_6$F$_5$)$_4$] cationic species (Scheme 2, path c) [25,26]. These two latter examples show that the allyl group is also more reactive than the borohydride one toward protic reagents. Finally, we checked that upon the addition of one equiv. of phenylsilane (d), the allyl signal of Nd(BH$_4$)$_2$(C$_3$H$_5$)(THF)$_x$ disappears while the borohydride resonances are maintained, even though the residual compound is not identified.

Clearly, this set of experiments allows the conclusion that, toward small-molecule insertion or acid/base reactions, the allyl group in the mixed Nd(BH$_4$)$_2$(C$_3$H$_5$)(THF)$_x$ compounds is more reactive than the borohydride, in sharp contrast to the reactivity observed in ring-opening polymerization. This prompted us to perform Density Functional Theory (DFT) calculations of the reaction mechanisms in order to shed light onto the reactivity difference between the borohydride and the allyl as active ligands for the ROP of ε-CL.

2.2. DFT Studies

For the sake of clarity, the study of the ROP of ε-CL mediated by the active ligands is separately analyzed in the following sections. The initiation step involving the allyl group is first discussed, followed by the initiation mediated by the borohydride ligands. Finally, the first propagation step is also investigated. The enthalpy profiles computed for the initiation step of the ROP of ε-CL with both initiator ligands are presented in Figure 1.

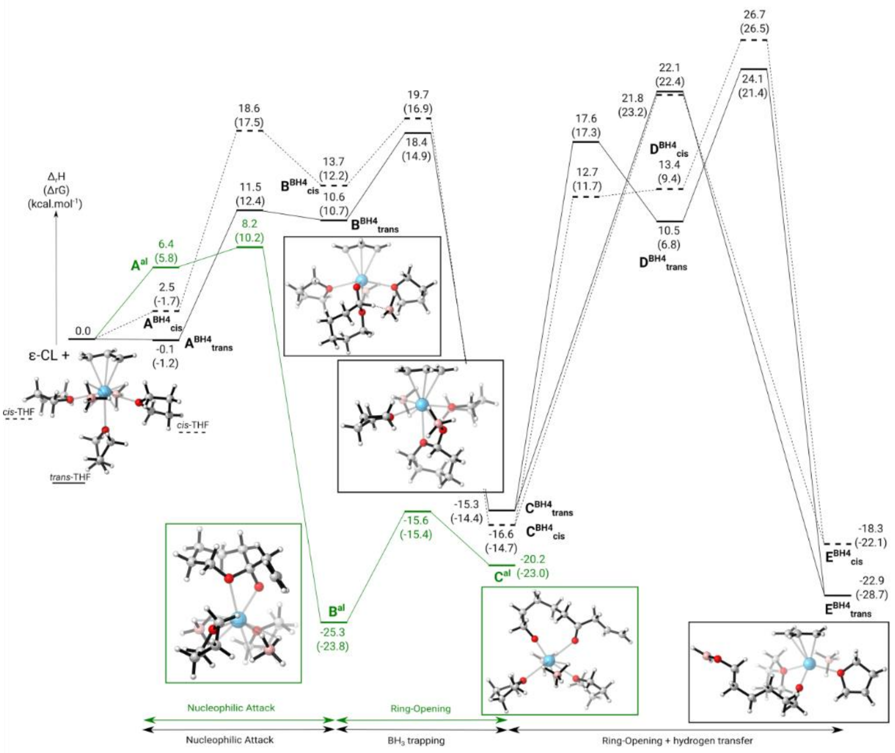

Figure 1. Calculated enthalpy profiles of the initiation step in the ROP of ε-CL mediated by the allyl group (green lines) or the borohydride group (black lines) of $La(BH_4)_2(C_3H_5)(THF)_3$. Black dotted lines: one of the THF molecules in the *cis* position to the allyl group is replaced by ε-CL. Black solid lines: the THF molecule in the *trans* position to the allyl group is replaced by ε-CL.

2.2.1. Allyl Initiation

On the allyl side, the ROP reaction proceeds via a coordination/insertion mechanism. Thus, the reaction begins by the formation of an endothermic ε-CL adduct, $\mathbf{A^{al}}$ (6.4 kcal·mol^{-1} with respect to the entrance channel). In this adduct, one of the THF molecules in the *cis* position, with respect to the allyl group, is replaced by ε-CL. The endothermicity of this adduct can be explained by the fact that ε-CL interacts with the metal center through its two oxygen atoms (exocyclic and endocyclic), forcing an η^3 to η^1 *hapticity change* of the allyl group. This adduct leads to a kinetically accessible transition state, which corresponds to the nucleophilic attack of the allyl group onto the carbonyl carbon of ε-CL, lying only 8.2 kcal·mol^{-1} above the separated reactants (1.8 kcal·mol^{-1} above the adduct). This transition state leads to a very stable intermediate, $\mathbf{B^{al}}$, located at −25.3 kcal mol^{-1} with respect to the separated reactants. It is interesting to note that, in this intermediate, the ε-CL ring remains closed (C-O distance of 1.495 Å), and the lanthanum atom is still interacting with two THF molecules and the two η^3-borohydride ligands. This system evolves to the acyl-oxygen bond cleavage transition state, i.e., the ring-opening, with a barrier of 9.7 kcal·mol^{-1} with respect to the previous intermediate (−15.6 kcal·mol^{-1} with respect to the separated reactants). This step corresponds to the rate-limiting step of the ROP initiation reaction of ε-CL mediated by the allyl ligand. This transition state leads to a final endothermic product (+5.1 kcal·mol^{-1}) with respect to the intermediate obtained after the nucleophilic attack of the allyl group but an exothermic one with respect to the entrance channel (−20.2 kcal·mol^{-1}), called $\mathbf{C^{al}}$. This makes this step loosely productive since the ring closure is kinetically more favorable than the ring-opening. It is interesting to note that in the final product, the endocyclic oxygen atom ensures not only the coordination to the metal center (La–O distance = 2.189 Å) but also the presence of an interaction between the metal center and the exocyclic oxygen (La–O distance = 2.640 Å). The relaxation of the growing polymer chain leading to the break of this interaction is endothermic by ca. 2.5 kcal·mol^{-1}. Thus, the initiation step involving the allyl group is kinetically accessible and thermodynamically favorable even if one of the intermediates is more stable than the final product.

2.2.2. Borohydride Initiation

On the borohydride side, the ROP reaction also proceeds via a coordination/insertion mechanism. In this case, the coordination of ε-CL to $La(BH_4)_2(C_3H_5)(THF)_3$ is followed by a hydride transfer to the ε-CL carbonyl carbon and the trapping of the borane molecule by the exocyclic carbonyl oxygen of the ε-CL. A second hydrogen transfer of the O-C(H)(R)-O···BH_3 group to the carbonyl carbon of the ε-CL leads to the cleavage of the acyl-oxygen bond and to the formation of an R–CH_2-O-BH_2 group, thus generating an alkoxyborane derivative $(BH_4)(C_3H_5)(THF)_2La–O(CH_2)_5CH_2OBH_2$. In this case, the reaction also starts with the formation of a first adduct in which one of the THF molecules is replaced by ε-CL. For the sake of clarity, only the most favorable possibility (represented as solid lines over dotted lines, Figure 1), i.e., involving the replacement of the THF molecule in the *trans* position to the allyl group by ε-CL, will be discussed. Subsequently, from this adduct, $\mathbf{A^{BH4}}_{\mathbf{trans}}$, the nucleophilic attack takes place via an accessible transition state, located at 11.5 kcal·mol^{-1} with respect to the separated reactants, yielding the first endothermic intermediate (10.6 kcal·mol^{-1} with respect to the entrance channel), $\mathbf{B^{BH4}}_{\mathbf{trans}}$. From a geometrical point of view, the hydrogen of the borohydride ligand has been totally transferred to the carbonyl carbon of ε-CL (C-H distance = 1.200 Å). In this intermediate, the borane molecule remains in interaction with the transferred hydrogen atom. From this unstable intermediate, the system easily reaches the second transition state corresponding to the trapping of the borane molecule by the exocyclic oxygen atom. This transition state lies 7.8 kcal mol^{-1} above the previous intermediate (18.4 kcal·mol^{-1} with respect to the separated reactants). As classically observed, the trapping occurs at long distances (H_3B-H distance = 2.446 Å and H_3B-O = 3.403 Å) and is driven by electrostatic interactions. The system evolves to a new highly exothermic intermediate (−15.3 kcal·mol^{-1} with respect to the entrance channel) in which the borane molecule is trapped by the exocyclic oxygen atom, $\mathbf{C^{BH4}}_{\mathbf{trans}}$. Finally, the formation of the R–CH_2-O-BH_2 terminal group can occur through a concerted pathway (hydrogen transfer + ring-opening) or through a multistep pathway (ring-opening followed by a second hydrogen transfer). In our case, as generally observed, the multistep pathway is higher in energy than the concerted one, 17.6 kcalmol^{-1} (ring-opening) and 24.1 kcalmol^{-1} (reduction process) vs. 22.1 kcal·mol^{-1}, with respect to the entrance channel. These transition states lead to the exothermic formation of the final alkoxyborane derivative, $\mathbf{E^{BH4}}_{\mathbf{trans}}$, which lies 22.9 kcal·mol^{-1} below the entrance channel. This step is thermodynamically favorable, making the overall ring-opening reaction thermodynamically possible. In this case, and contrary to the allyl product, the alkoxyborane chain is fully linear, with the decoordination of the exocyclic oxygen atom from the metal center.

In summary, both initiation reactions are possible. However, the overall formation of an alkoxyborane growing chain is slightly more favorable than the alkoxide chain with an allyl as the end-group, −20.2 (allyl) vs. −22.9 kcal·mol^{-1} (borohydride). From a kinetic point of view: (i) when the nucleophilic attack involves the allyl group, the rate-determining step corresponds to the ring-opening step with an activation barrier of 9.7 kcal·mol^{-1}; (ii) in the case of the borohydride group, the rate-determining step corresponds to the concerted pathway with an activation barrier of 37.4 kcal·mol^{-1}. Thus, the formation of the alkoxide chain with an allyl as the end-group is kinetically preferred over the formation of an alkoxyborane growing chain. Therefore, the allyl would afford the kinetic product, whereas the borohydride leads to the thermodynamic one. The next insertion was therefore investigated to corroborate our findings.

2.2.3. Propagation Step

In order to get a better insight into the reactivity difference between the borohydride and the allyl groups as active ligands for the ROP of ε-CL, the first propagation step, namely, the second ε-CL insertion, was investigated. For this second step, we have only considered the possible reactions after the formation of a growing chain with an allyl as the end-group. The enthalpy profiles computed for this step are presented in Figure 2. Starting from the complex $La(BH_4)_2(OC_5H_{10}COC_3H_5)(THF)_2$, the calculated reaction profile supports the idea that the alkoxide undergoes a nucleophilic attack onto the carbonyl carbon of the second ε-CL monomer, and a subsequent ring-opening generates the final $La(BH_4)_2(OC_5H_{10}COOC_5H_{10}COC_3H_5)(THF)_2$ complex, $\mathbf{F^{al}}$. With respect to $La(BH_4)_2(OC_5H_{10}COC_3H_5)(THF)_2$, this second insertion is thermodynamically favorable (by 2.4 kcal·mol^{-1}). The activation barriers for the nucleophilic attack and the ring-opening are low and similar (ca. 5 kcal·mol^{-1}). At this second insertion stage, a nucleophilic attack can also be done by one of the two borohydrides onto the ε-CL carbonyl carbon. This mechanism is very similar to that of the initiation step, as discussed in the previous section. It is interesting to note that no significant difference (less than 3 kcal·mol^{-1}) is observed concerning the stability of the intermediates and the activation barriers between the initiation and this propagation step. From a geometric point of view, the structures of the different intermediates and transition states are also similar.

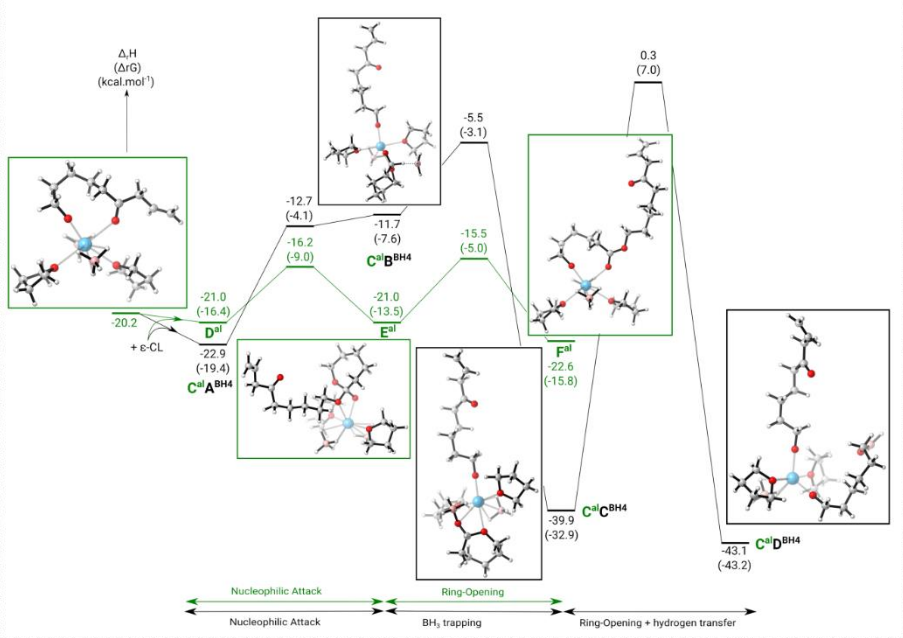

Figure 2. Calculated enthalpy profiles of the first propagation step in the ROP of ε-CL mediated by the allyl group (green lines) or the borohydride group (black lines) of $La(BH_4)_2(OC_5H_{10}COC_3H_5)(THF)_2$.

In conclusion, from a kinetic point of view, there is a clear preference for the alkoxide nucleophilic attack. However, whereas this second step is kinetically favorable, from a thermodynamic point of view, the formed product remains, as for the initiation reaction, less stable than the intermediate obtained after the first nucleophilic attack of the allyl group, −25.3 vs. −22.6 kcal·mol^{-1}. Thus, even if the activation barriers are accessible, the allyl group is not active for the ROP of ε-CL due to the formation of this highly stable intermediate that disfavors the subsequent ring-opening. On the other hand, the ROP of ε-CL mediated by the borohydride ligands is less favorable from a kinetic point of view, but the insertion of the monomers is thermodynamically favorable. This confirms and rationalizes the results previously obtained at the laboratory scale.

In contrast to the ROP reactivity, the higher nucleophilicity of the allyl group over the borohydride one in the simple cases of insertion and acid/base reactions with small molecular substrates is highlighted thanks to ^{1}H NMR experiments.

3. Materials and Methods

3.1. Experimental

All manipulations were performed under an inert atmosphere using Schlenk techniques, or in a dry solvent-free glovebox (Jacomex $O_2 < 1$ ppm, $H_2O < 4$ ppm). The solvents for synthesis (THF and toluene) were dried over sodium/benzophenone ketyl, degassed and stored in solvent pots under static vacuum. C_6D_6 and d_8-THF were dried over NaK. $RE(BH_4)_3(THF)_{2–3}$ (La, Nd, Sm, Y and Sc) compounds were prepared as reported [1,2]. Benzophenone (Aldrich, 99%) was purified by crystallization. Tetramethylcyclopentadiene, tetramethylethylcyclopentadiene and phenylsilane (Aldrich) were dried over molecular sieves. Dimethylanilinium tetraphenylborate (Aldrich) was used as received. Technical grade L-LA (Aldrich) was purified by two subsequent recrystallizations in hot toluene followed by sublimation. ε-Caprolactone (Aldrich) was dried over calcium hydride, distilled twice and stored over molecular sieves (3 Å) in a glovebox. ^{1}H NMR spectra were recorded on a Bruker Avance 300 instrument at 300 K. All ^{1}H chemical shifts (reported in ppm) were determined using residual signals of the deuterated solvents.

3.2. NMR Monitoring Experiments

Reactivity of $Sc(BH_4)_2(C_3H_5)(THF)_{2.5}$ with benzophenone: $[D_8]$THF (0.5 mL) was added through distillation to $Sc(BH_4)_2(allyl)(THF)_{2.5}$ (4 mg, 14 µmol) and benzophenone (2.5 mg, 14 µmol) in an NMR tube equipped with a Teflon valve. ^{1}H NMR spectroscopy of the greenish-brown solution was recorded after 3 h. ^{1}H NMR ($[D_8]$THF, 300 MHz, 20 °C): δ 7.45–7.11 (phenyl rings, 10H), 5.91 (m, 1H, CH_δ); 5.05 (m, 1H, CH_β); 4.92 (m, 1H, CH_γ); 3.08 (m, 2H, $2CH_\alpha$); 0.39 (BH_4).

Reactivity of $Y(BH_4)_2(C_3H_5)(THF)_3$ with benzophenone: $[D_8]$THF (0.5 mL) was added through distillation to $Y(BH_4)_2(allyl)(THF)_3$ (5.1 mg,14 µmol) and benzophenone (2.5 mg, 14 µmol) in an NMR tube equipped with a Teflon valve. ^{1}H NMR spectroscopy of the colourless solution was recorded after 3 h. ^{1}H NMR ($[D_8]$THF, 300 MHz, 20 °C): δ 7.45 (o-C_6H_5); 7.14 (m-C_6H_5); 7.01 (p-C_6H_5); 5.88 (m, 1H, CH_δ); 4.88 (m, 1H, CH_β); 4.75 (m, 1H, CH_γ); 3.13 (m, 2H, $2CH_\alpha$); 0.423 (BH_4).

Reactivity of $La(BH_4)_2(C_3H_5)(THF)_3$ with benzophenone: $[D_8]$THF (0.5 mL) was added through distillation to $La(BH_4)_2(allyl)(THF)_3$ (5.8 mg,14 µmol) and benzophenone (2.5 mg, 14 µmol) in an NMR tube equipped with a Teflon valve. ^{1}H NMR spectroscopy of the orange-brown solution was recorded after 3 h. ^{1}H NMR ($[D_8]$THF, 300 MHz, 20 °C): δ 7.43 (o-C_6H_5); 7.14 (m-C_6H_5); 7.02 (p-C_6H_5); 5.84 (m, 1H, CH_δ); 4.91 (m, 1H, CH_β); 4.79 (m, 1H, CH_γ); 3.07 (m, 2H, $2H_\alpha$); 0.85 (BH_4).

Reactivity of $Nd(BH_4)_2(C_3H_5)(THF)_4$ with HC_5Me_4H: $[D_6]$benzene (0.5 mL) was added to C_5Me_4H (1.4 µL, 9 µmol) in an NMR tube equipped with a Teflon valve followed by the addition of $Nd(BH_4)_2(C_3H_5)(THF)_4$ (4.7 mg, 9 µmol). ^{1}H NMR spectroscopy of the light green solution was recorded after 1 day. ^{1}H NMR ($[D_6]$benzene, 300 MHz, 20 °C): δ 92.6 (br. s, BH_4); 9.36 (s, 6H, $2CH_3$); 7.56 (s, 6H, $2CH_3$); 5.71 (m, 1H, CH); 4.97 (m, 2H, CH_2); 1.54 (m, 3H, CH_3); −0.70 (s, THF); −1.86 (s, THF).

Reactivity of $Nd(BH_4)_2(C_3H_5)(THF)_4$ with $HC_5Me_4(CH_2CH_3)$: $[D_6]$benzene (0.5 mL) was added to $C_5Me_4(CH_2CH_3)$(1.5 µL, 8 µmol) in an NMR tube equipped with a Teflon valve followed by the addition of $Nd(BH_4)_2(C_3H_5)(THF)_4$ (4.2 mg, 8 µmol). ^{1}H NMR spectroscopy of the light green solution was recorded after 1 day. ^{1}H NMR ($[D_6]$benzene, 300 MHz, 20 °C): δ 96.2 (br. s, BH_4); 8.62 (s, 6H, $2CH_3$); 8.22 (s, 6H, $2CH_3$); 6.76 (m, 2H, CH_2); 5.71 (m, 1H, CH); 4.97 (m, 2H, CH_2); 2.64 (m, 3H, CH_3); 1.55 (m, 3H, CH_3); −0.79 (s, THF); −2.41 (s, THF).

Reactivity of $Nd(BH_4)_2(C_3H_5)(THF)_4$ with $[HNMe_2Ph][B(C_6F_5)_4]$: $Nd(BH_4)_2(C_3H_5)(THF)_4$ (5 mg, 10 µmol) was dissolved in $[D_8]$THF (0.5 mL) in an NMR tube equipped with a Teflon valve. One equivalent of $[HNMe_2Ph][B(C_6F_5)_4]$ (8 mg) was added and a reaction instantaneously occurred with the formation of bubbles. ^{1}H NMR spectroscopy of the light blue solution displayed the signals of the known complex $[Nd(BH_4)_2(THF)_5][B(C_6F_5)_4]$ [26].

Reactivity of $Nd(BH_4)_2(C_3H_5)(THF)_4$ with phenylsilane: $Nd(BH_4)_2(C_3H_5)(THF)_4$ (6 mg, 12 µmol) was added in an NMR tube equipped with a Teflon valve followed by $[D_6]$benzene (0.5 mL) in a glovebox. $PhSiH_3$ (1.5 µL, 12 µmol) was added, and the ^{1}H NMR spectrum of the green solution was recorded after 20 h. One more equivalent of phenylsilane (1.5 µL, 12 µmol) was added, and the tube was heated at 50 °C for 6 days. This resulted in a yellow solution with brown precipitate. ^{1}H NMR ($[D_6]$benzene, 300 MHz, 20 °C): δ 99.4 (br s, BH_4); 7.38–7.10 (m, phenyl rings); 5.74 (m); 4.97 (m); 4.51 (m); 4.23 (s, Si-H); 3.90 (s); 3.5 (s); 2.33 (br s, THF); 1.17 (br s, THF). Assignment of signals in detail could not be performed due to the paramagnetism of neodymium (III).

3.3. Methodological Details

All the DFT calculations were performed with Gaussian 09 [27]. Calculations were carried out at the DFT level of theory using the hybrid functional B3PW91 [28–32]. Geometry optimizations were achieved without any symmetry restriction. Vibrational frequencies were systematically computed in order to characterize the nature of the stationary points. The Stuttgart effective core potentials [33,34] and their associated basis sets were used for lanthanum. For the La atom, the basis sets were augmented by a set of polarization functions (ζf = 1.0 for La). The H, B, C and O atoms were treated with 6–31G(d,p) double ζ basis sets [35]. The electron density and partial charge distribution were examined in terms of localized electron-pair bonding units using the NBO program [36,37].

4. Conclusions

In this paper, the activity of the nucleophilic ligand, allyl vs. borohydride, in the two first steps (initiation and first propagation) of the ROP of ε-caprolactone mediated by $La(BH_4)_2(C_3H_5)(THF)_3$ is investigated. This study highlights that even if, from the kinetic point of view, there is a preference for the ROP of ε-CL mediated by the allyl ligand, this ligand is not active due to the low stability of the inserted products. On the other hand, the ε-caprolactone ROP with the borohydride ligand is more energetically costly but thermodynamically favorable. Thus, on $La(BH_4)_2(C_3H_5)(THF)_3$, only the borohydride ligands are active for the ROP of ε-CL.

Supplementary Materials: The following are available online at http://www.mdpi.com/2073-4344/10/8/820/s1, Figure S1: MALDI-ToF mass spectrum of polylactide synthesized with $Nd(BH_4)_2(C_3H_5)(THF)_3$. Figure S2: MALDI-ToF mass spectrum of polylactide synthesized with $Y(BH_4)_2(C_3H_5)(THF)_3$. Computational data as a xyz file.

Author Contributions: Conceptualization, M.V., F.B. and L.M.; software, L.M., I.D.R.; formal analysis, S.F., J.J.; data curation, M.V., F.B., L.M., I.D.R., S.F., J.J.; writing—review and editing, M.V., F.B., L.M., I.D.R.; supervision, M.V., F.B. All authors have read and agreed to the published version of the manuscript.

Funding: The authors would like to thank CNRS and Région Hauts de France for funding.

Acknowledgments: The authors would like to thank François Stoffelbach for Maldi-ToF analysis. L.M. is a member of the Institut Universitaire de France. This work was performed using HPC resources from CALMIP (Grant 2016-p0833).

Conflicts of Interest: The authors declare no conflict of interest.

References

1. Fadlallah, S.; Terrier, M.; Jones, C.; Roussel, P.; Bonnet, F.; Visseaux, M. Mixed Allyl–Borohydride Lanthanide Complexes: Synthesis of $Ln(BH_4)_2(C_3H_5)(THF)_3$ (Ln = Nd, Sm), Characterization, and Reactivity toward Polymerization. *Organometallics* **2016**, *35*, 456–461. [CrossRef]

2. Fadlallah, S.; Jothieswaran, J.; Capet, F.; Bonnet, F.; Visseaux, M. Mixed Allyl Rare-Earth Borohydride Complexes: Synthesis, Structure, and Application in (Co-)Polymerization Catalysis of Cyclic Esters. *Chem. Eur. J.* **2017**, *23*, 15644–15654. [CrossRef]
3. Guillaume, S.M.; Maron, L.; Roesky, P.W. Catalytic Behavior of Rare-Earth Borohydride Complexes in Polymerization of Polar Monomers. In *Handbook on the Physics and Chemistry of Rare Earths*; Bünzli, J.-C.G., Pecharsky, V.K., Eds.; Elsevier: Amsterdam, The Netherlands, 2014; Volume 244, pp. 1–86.
4. Guillaume, S.M.; Schappacher, M.; Soum, A. Polymerization of ε-Caprolactone Initiated by $Nd(BH_4)_3(THF)_3$: Synthesis of Hydroxytelechelic Poly(ε-caprolactone). *Macromolecules* **2003**, *36*, 54–60. [CrossRef]
5. Bonnet, F.; Cowley, A.R.; Mountford, P. Lanthanide Borohydride Complexes Supported by Diaminobis(phenoxide) Ligands for the Polymerization of ε-Caprolactone and l- and rac-Lactide. *Inorg. Chem.* **2005**, *44*, 9046–9055. [CrossRef] [PubMed]
6. Nakayama, Y.; Okuda, S.; Yasuda, H.; Shiono, T. Synthesis of multiblock poly(L-lactide)-*co*-poly(ε-caprolactone) from hydroxy-telechelic prepolymers prepared by using neodymium tetrahydroborate. *React. Funct. Polym.* **2007**, *67*, 798–806. [CrossRef]
7. Hu, C.; Louisy, E.; Fontaine, G.; Bonnet, F.J. Cyclic versus linear polylactide: Straightforward access using a single catalyst. *Polym. Sci. Part A Polym. Chem.* **2017**, *55*, 3175–3179. [CrossRef]
8. Visseaux, M.; Bonnet, F. Borohydride complexes of rare earths, and their applications in various organic transformations. *Coord. Chem. Rev.* **2011**, *255*, 374–420. [CrossRef]
9. Lyubov, D.M.; Tolpygin, A.O.; Trifonov, A.A. Rare-earth metal complexes as catalysts for ring-opening polymerization of cyclic esters. *Coord. Chem. Rev.* **2019**, *392*, 83–145. [CrossRef]
10. Palard, I.; Soum, A.; Guillaume, S.M. Rare Earth Metal Tris(borohydride) Complexes as Initiators for ε-Caprolactone Polymerization: General Features and IR Investigations of the Process. *Macromolecules* **2005**, *38*, 6888–6894. [CrossRef]
11. Barros, N.; Mountford, P.; Guillaume, S.M.; Maron, L. A DFT Study of the Mechanism of Polymerization of ε-Caprolactone Initiated by Organolanthanide Borohydride Complexes. *Chem. Eur. J.* **2008**, *14*, 5507–5518. [CrossRef]
12. Jenter, J.; Roesky, P.W.; Ajellal, N.; Guillaume, S.M.; Susperregui, N.; Maron, L. Bis(phosphinimino)methanide Borohydride Complexes of the Rare-Earth Elements as Initiators for the Ring-Opening Polymerization of ε-Caprolactone: Combined Experimental and Computational Investigations. *Chem. Eur. J.* **2010**, *16*, 4629–4638. [CrossRef]
13. Skvortsov, G.G.; Yakovenko, M.V.; Castro, P.M.; Fukin, G.K.; Cherkasov, A.V.; Carpentier, J.-F.; Trifonov, A.A. Lanthanide Borohydride Complexes of Bulky Guanidinate Ligands $[(Me_3Si)_2NC(N\text{-}Cy)_2]_2Ln(\mu\text{-}BH_4)_2Li(THF)_2$ (Ln = Nd, Sm, Yb): Synthesis, Structure and Catalytic Activity in Lactide Polymerization. *Eur. J. Inorg. Chem.* **2007**, 3260–3267. [CrossRef]
14. Dyer, H.E.; Huijser, S.; Susperregui, N.; Bonnet, F.; Schwarz, A.D.; Duchateau, R.; Maron, L.; Mountford, P. Ring-Opening Polymerization of rac-Lactide by Bis(phenolate)amine-Supported Samarium Borohydride Complexes: An Experimental and DFT Study. *Organometallics* **2010**, *29*, 3602–3621. [CrossRef]
15. Bonnet, F.; Stoffelbach, F.; Fontaine, G.; Bourbigot, S. Continuous cyclo-polymerization of l-lactide by reactive extrusion using atoxic metal-based catalysts: Easy access to well-defined polylactide macrocycles. *RSC Adv.* **2015**, *5*, 31303–31310. [CrossRef]
16. Woodman, T.J.; Schormann, M.; Hughes, D.L.; Bochmann, M. New Bulky Allyl Complexes of Lanthanide Metals: Role of Alkali-Metal Cations in Controlling Solid-State and Solution Assemblies in Precatalysts. *Organometallics* **2003**, *22*, 3028–3030. [CrossRef]
17. Barbier-Baudry, D.; Bonnet, F.; Dormond, A.; Finot, E.; Visseaux, M. Diene/polar monomer copolymers, compatibilisers for polar/non-polar polymer blends. A controlled block copolymerization with a single-site component samarocene initiator. *Macromol. Chem. Phys.* **2002**, *203*, 1194–1200. [CrossRef]
18. Woodman, T.J.; Schormann, M.; Hughes, D.L.; Bochmann, M. Sterically Hindered Lanthanide Allyl Complexes and Their Use as Single-Component Catalysts for the Polymerization of Methyl Methacrylate and ε-Caprolactone. *Organometallics* **2004**, *23*, 2972–2979. [CrossRef]
19. Sánchez-Barba, L.F.; Hughes, D.L.; Humphrey, S.M.; Bochmann, M. Ligand Transfer Reactions of Mixed-Metal Lanthanide/Magnesium Allyl Complexes with β-Diketimines: Synthesis, Structures, and Ring-Opening Polymerization Catalysis. *Organometallics* **2006**, *25*, 1012–1020. [CrossRef]

20. Susperregui, N.; Kramer, M.U.; Okuda, J.; Maron, L. Theoretical Study on the Ring-Opening Polymerization of ε-Caprolactone by $[YMeX(THF)_5]^+$ with X = BH_4, NMe_2. *Organometallics* **2011**, *30*, 1326–1333. [CrossRef]
21. Kramer, M.; Robert, D.; Arndt, S.; Zeimentz, P.M.; Spaniol, T.P.; Yahia, A.; Maron, L.; Eisenstein, O.; Okuda, J. Cationic Methyl Complexes of the Rare-Earth Metals: An Experimental and Computational Study on Synthesis, Structure, and Reactivity. *Inorg. Chem.* **2008**, 9265–9278. [CrossRef]
22. Robert, D.; Abinet, E.; Spaniol, T.P.; Okuda, J. Cationic Allyl Complexes of the Rare-Earth Metals: Synthesis, Structural Characterization, and 1,3-Butadiene Polymerization Catalysis. *Chem. Eur. J.* **2009**, *15*, 11937–11947. [CrossRef]
23. Visseaux, M.; Baudry, D.; Dormond, A.; Qian, C. Co-ordinatively unsaturated neodymium hydrides, stability in solution. *J. Organomet. Chem.* **1999**, *574*, 213–218. [CrossRef]
24. Bonnet, F.; Visseaux, M.; Barbier-Baudry, D.; Hafid, A.; Vigier, E.; Kubicki, M.M. Organometallic Early Lanthanide Clusters: Syntheses and X-ray Structures of New Monocyclopentadienyl Complexes. *Inorg. Chem.* **2004**, *43*, 3682–3690. [CrossRef]
25. Robert, D.; Kondracka, M.; Okuda, J. Cationic rare-earth metal bis(tetrahydridoborato) complexes: Direct synthesis, structure and ring-opening polymerization activity toward cyclic esters. *Dalton Trans.* **2008**, 2667–2669. [CrossRef]
26. Visseaux, M.; Mainil, M.; Terrier, M.; Mortreux, A.; Roussel, P.; Mathivet, T.; Destarac, M. Cationic borohydrido–neodymium complex: Synthesis, characterization and its application as an efficient pre-catalyst for isoprene polymerization. *Dalton Trans.* **2008**, *34*, 4558–4561. [CrossRef]
27. Frisch, M.J.; Trucks, G.W.; Schlegel, H.B.; Scuseria, G.E.; Robb, M.A.; Cheeseman, J.R.; Scalmani, G.; Barone, V.; Petersson, G.A.; Nakatsuji, H.; et al. *Gaussian 09, Revision D.01*; Gaussian Inc.: Wallingford, CT, USA, 2016.
28. Perdew, J.P.; Chevary, J.A.; Vosko, S.H.; Jackson, K.A.; Pederson, M.R.; Singh, D.J.; Fiolhais, C. Erratum: Atoms, molecules, solids, and surfaces: Applications of the generalized gradient approximation for exchange and correlation. *Phys. Rev. B* **1993**, *48*, 4978. [CrossRef]
29. Perdew, J.P.; Burke, K.; Wang, Y. Erratum: Generalized gradient approximation for the exchange-correlation hole of a many-electron system. *Phys. Rev. B* **1998**, *57*, 14999–15033. [CrossRef]
30. Perdew, J.P.; Chevary, J.A.; Vosko, S.H.; Jackson, K.A.; Pederson, M.R.; Singh, D.J.; Fiolhais, C. Atoms, molecules, solids, and surfaces: Applications of the generalized gradient approximation for exchange and correlation. *Phys. Rev. B* **1992**, *46*, 6671–6687. [CrossRef]
31. Perdew, J.P.; Burke, K.; Wang, Y. Generalized gradient approximation for the exchange-correlation hole of a many-electron system. *Phys. Rev. B* **1996**, *54*, 16533–16539. [CrossRef]
32. Perdew, J.P. *Unified Theory of Exchange and Correlation beyond the Local Densityapproximation*; Akademie Verlag: Berlin, Germany, 1991; Volume 11.
33. Dolg, M.; Stoll, H.; Preuss, H. Energy-adjusted ab initio pseudopotentials for the rare earth elements. *J. Chem. Phys.* **1989**, *90*, 1730–1734. [CrossRef]
34. Cao, X.; Dolg, M. Segmented contraction scheme for small-core lanthanide pseudopotential basis sets. *J. Mol. Struct.* **2002**, *581*, 139–147. [CrossRef]
35. Pople, P.C.; Hariharan, J.A. The influence of polarization functions on molecular orbital hydrogenation energies. *Theor. Chim. Acta* **1973**, *28*, 213–222.
36. Reed, A.E.; Curtiss, L.A.; Weinhold, F. Intermolecular interactions from a natural bond orbital, donor-acceptor viewpoint. *Chem. Rev.* **1988**, *88*, 899–926. [CrossRef]
37. Reed, A.E.; Weinhold, F. Natural bond orbital analysis of near-Hartree–Fock water dimer. *J. Chem. Phys.* **1983**, *78*, 4066–4073. [CrossRef]